Towards a direct dating of fault gouges using luminescence dating techniques – Methodological aspects

D. Banerjee*[,§], A. K. Singhvi*[,†], Kanchan Pande*, V. D. Gogte[‡] and B. P. Chandra[#]

*Physical Research Laboratory, Ahmedabad 380 009, India
[‡]Deccan College, Postgraduate and Research Institute, Pune 400 006, India
[#]Department of Physics, Rani Durgavati Vishwavidyalaya, Jabalpur 482 001, India
[§]Present address: School of Geosciences, University of Geosciences, Wollongong University, New South Wales, Australia

Results of a study to date neotectonic movements and past seismic events in Himalaya using the thermoluminescence technique are described. The basic assumption of *zeroing* of geological thermoluminescence during faulting was examined using techniques such as mechanoluminescence and clay mineralogy. Variation of the luminescence paleodoses with grain-size and the paleodose of the rocks away from the fault zone were also examined. The results indicate that neotectonic activity took place around 40 ka ago along Nainital and Sleepy Hollow fault, 70 ka ago along the MBT and 60 ka along the Mohand thrust. In conjunction with other evidences from the lacustrine records in the region, phases of regionally extended tectonic activities at about 40 ka and 60 ka are inferred.

SEDIMENTARY strata in Himalaya are being continuously stressed due to an ongoing northward movement of the Indian plate. Such stresses are released periodically and induce earthquakes and neotectonic activity along the faults. The concept of locked segments has been developed to assess the seismogenic potential of a region. This relates to the build-up of stress(es) and their release. It is, however, yet to be established if the accumulation of such stresses and their release as neotectonic movements along faults have any definite periodicity. This is an aspect crucial towards providing a boundary condition for geophysical modelling of such processes.

In the Indian context, studies on the chronology of such paleoseismic events have been limited (Sukhija, pers. commun.). In general, there is a paucity of samples that can be unambiguously correlated to neotectonic movements or paleoseismic events and can be used for radiometric dating. Historical records are also limited to scattered descriptions spanning only the past few centuries. With this perspective, an effort was made to develop luminescence dating techniques for direct dating of fault gouges and deformed sedimentary structures[1,2].

[†]For correspondence. (e-mail: singhvi@prl.ernet.in)

A basic advantage of this application is the fact that fault gouge, is formed by brittle fracturing of rocks as a result of slip along the faults, is itself used for dating. Thus, in a well-mapped fault zone region, there is an unambiguous association between sample and the event being dated. The dating application assumes that during the faulting event, the luminescence intensity of the gouge material is 'zeroed' and subsequent to the faulting event, the thermal regimes were such that no loss of signal occurred on storage. This premise was central to the present study. In the present article, results of studies aimed at establishing the 'zeroing' of previously stored luminescence signal during faulting are described. The application closely parallels the application of electron spin resonance for the dating of faults initiated by Ikeya *et al.*[3] to date the Atotsugawa Fault, Japan. Differences in measurement sensitivities between luminescence and ESR measurements and in saturation levels suggest that the two methods would provide a complementary dating range spanning a few centuries to a few million years in favourable situations.

Luminescence dating

The first attempts to date paleoearthquakes using thermoluminescence (TL) dating were based on luminescence dating of buried soils that were originally formed on colluvial debris. The basic premise was that during soil formation, bioturbation of the surface layers of the colluvial debris resulted in a onsite sun-exposure of the constituent mineral, thereby resetting their thermoluminescence clock. Forman *et al.*[4,5] excavated trenches across fault scarps from the American Fork segment of the Wasatch Fault zone. Buried soils sandwiched between colluvium, faulted loess and sag pond deposits were dated using TL. The results were consistent with those provided by radiocarbon dating of soil organic matter. No effort was made on the luminescence dating of fault gouges until the first systematic dating effort by

Singhvi *et al.*[1]. The present contribution is an extension of this study and discusses its implications on the dating of neotectonic events in the Himalaya.

The method

Luminescence dating of fault gouges is based on the premise that during faulting, the geological luminescence of minerals constituting the fault gouge is reduced to a zero level due to frictional heating and/or cataclastic deformation. It is assumed that sufficient heat energy of deformation energy is available to detrap the trapped changes that eventually participate in the luminescence process. Subsequently, the luminescence signal builds up due to irradiation by ambient natural radioactivity (U, Th, K) such that at the time of sample excavation, the age of faulting event is given by the expression,

luminescence age = luminescence acquired since faulting/annual rate of luminescence acquisition.

As the luminescence is induced by natural radiation field around the sample, the above equation can be expressed in radiation dose units such that the age equation becomes,

age = (paleodose/annual dose),

where paleodose (P) is the laboratory beta dose that induces a luminescence intensity identical to that in a virgin (natural) sample. Annual dose is defined as the annual radiation exposure of the sample from the decay of naturally occurring radionuclides and cosmic rays. Thus, in order to find the luminescence age of faulting, estimation of paleodose and annual dose is needed. A luminescence age represents the most recent, climatic movement occurring in the fault zone. The technique is preferred to other radiometric techniques because of several reasons of ubiquity of gouge in fault zones in comparison to organics and a dating range of 1–200 ka. Further, the luminescence ages are calendar ages and, as a consequence, no calibration to calendar years is needed.

A major concern in the present study was to assume 'zeroing event' as the reliability of luminescence ages depended crucially on the validity of this assumption. As detailed below, several experiments were carried out to test this basic assumption.

Fault zone models

On the basis of rock deformation experiments, study of structures in deeply exhumed fault zones and the distribution of earthquakes, fault zone models have been developed[6,7]. In the model proposed by Scholz[7], rocks in the upper 11 km undergo cataclastic deformation (displacement within and between grains). Rock strength, as measured by resistance to frictional sliding, increases with depth, due to its dependence on confining pressure. The deepest strata in this zone can store the maximum amount of strain energy, and are therefore the focal point of most earthquakes. This is supported by the fact that during an earthquake, a majority of the mainshocks occur in this zone.

At depths below ~15 km, plastic/ducticle deformation is the dominant mechanism. Rock strength decreases with increasing depth and temperature. This is in contrast to its behaviour in the upper regions of the crust. Thus, the strain energy cannot be accumulated implying aseismic deformation with the absence of earthquakes. It needs to be mentioned here that this brittle-plastic transition zone depends on rock type, and is deepest for mantle materials, and shallowest for granitic crust.

Another aspect that needs consideration is the presence of interstitial water in fault zones. This causes a reduction in the confining pressure and results in weakening the fault. Frictional resistance is thus easily overcome compared to dry rocks and aseismic deformation may be prevalent in such a situation.

Implications on luminescence ages

As discussed above, ages determined using luminescence techniques will be accurate provided the luminescence signals of the mineral grains have been reset thermally or by the effect of confining pressure and local shear stresses. Luminescence techniques will generally be applicable to both the brittle and plastic deformation zones as long as the above criterion of *zeroing* is satisfied; however, the interpretation of the ages will be different. While ages in the brittle zone will relate to faulting or the earthquake event, age of ductile deformation events will most likely relate to other deformation episodes. In the present study the efforts in this study were directed towards dating rocky materials within the brittle zones.

Site and sample details

For the present studies, fault gouges were collected from the seismically active Himalayan belt. In general, the samples were collected after digging a trench of 1–2 m size. A brief description of these sites along with a general geological framework is given below.

Geophysical and structural studies suggest that seismicity in the Himalaya is related to movements along three major longitudinal thrusts/faults (Figure 1), viz.

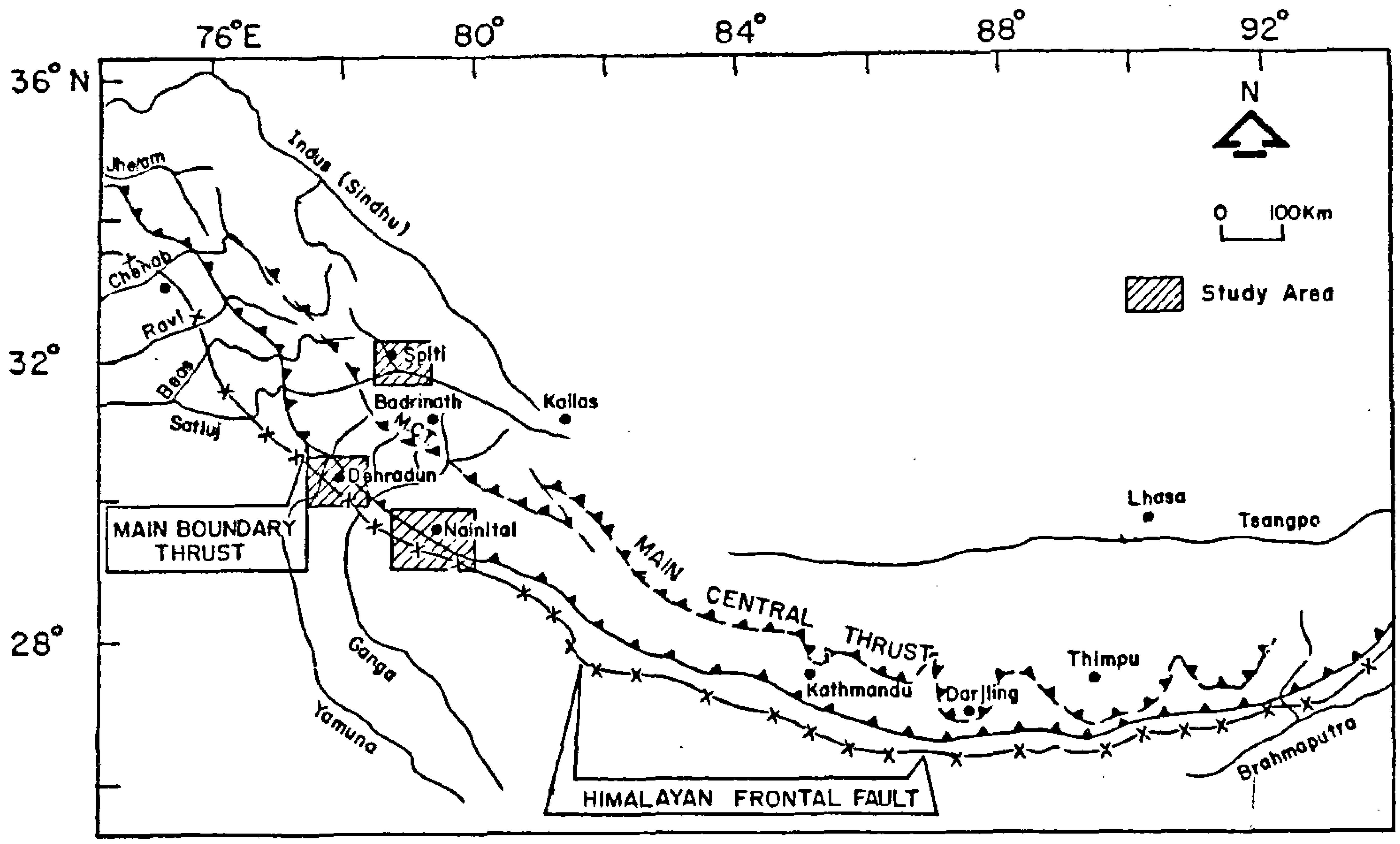

Figure 1. Generalized tectonic map of the Himalaya showing the three major east-west trending thrusts/faults. The shaded rectangles indicate sampling locations taken up for the TL/IRSL dating by PRL.

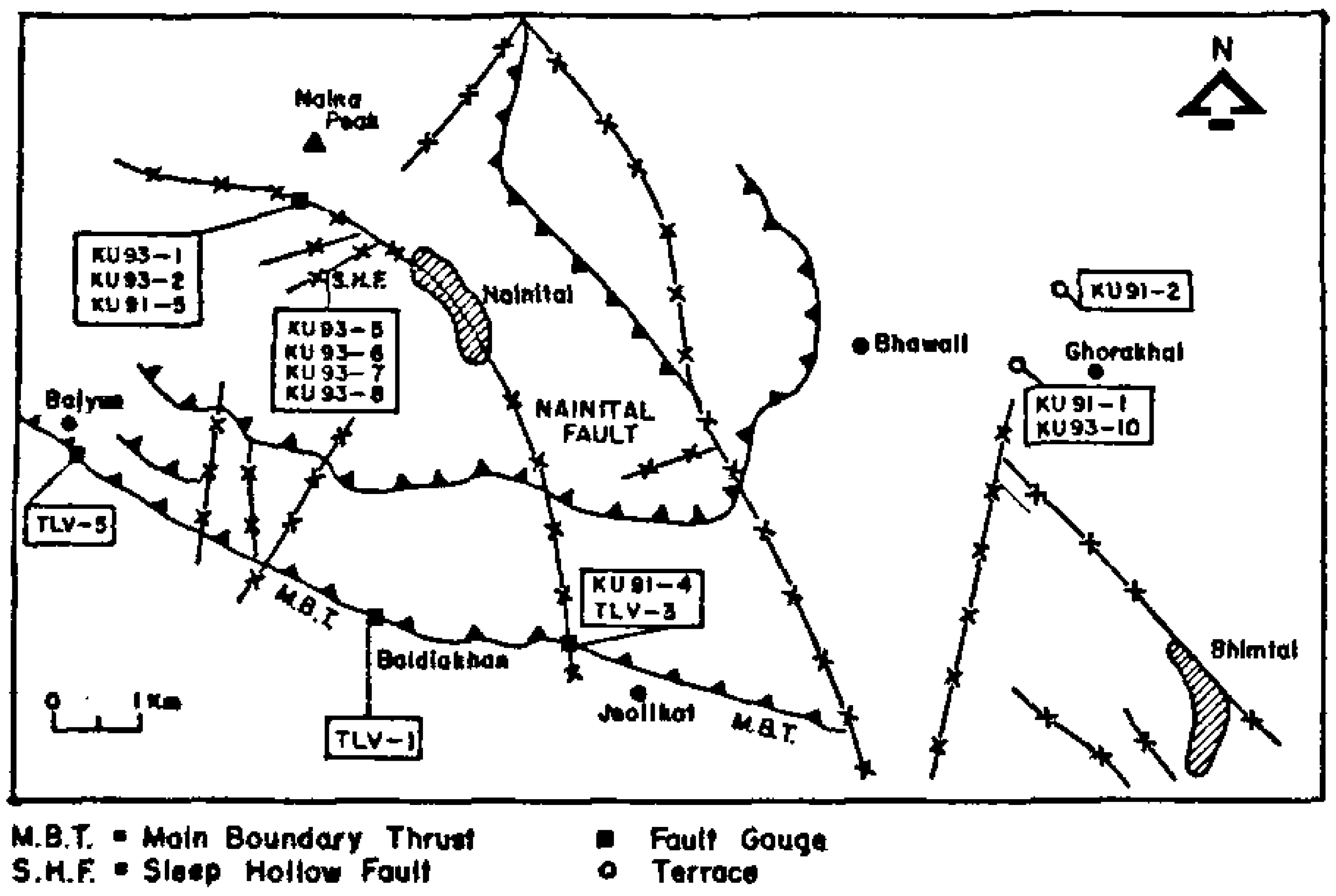

Figure 2. Tectonic map around Nainital indicating the sampling locations.

the Himalayan Frontal Fault (HFF), the Main Boundary Thrust (MBT) and the Main Central Thrust (MCT). These thrusts divide the Himalaya into three lithotectonic zones which are further dissected by numerous transverse faults[8]. After cessation of movements along the Indus Suture Zone, the continued movement of the Indian plate has resulted in the breaking up of the Indian crust along MCT, MBT and HFF[7]. Presently, the most active tectonic zone is HFF. Fault gouges for luminescence dating (thermoluminescence (TL) and infrared stimulated luminescence (IRSL)) were collected from MBT (in the Nainital region), Sleepy Hollow Fault, Nainital Fault (Figure 2) and Mohand Thrust (Figure 3). The host rocks in the Nainital Fault and Sleepy Hollow Fault were shales and, sandstones and sedimentary shales along the Main Boundary Thrust and the Mohand Thrust. A brief description of these sites is provided below.

MBT

MBT (Figures 1 and 2) is a chain of steeply inclined thrusts which divide the outer Himalayan Siwalik belt from the older, mature, recently rejuvenated Lesser Himalaya[9]. Various evidences provided by Valdiya[9] indicate neotectonic activity along MBT. These include, (a) presence of wide valleys comprising cones and fans of landslide debris, (b) unpaired fluvial terraces overlapped by landslide debris, (c) uplifts and offsets of stream terraces, (d) evolution of sharp scarps, (e) warping and fitting of rocks/sediments and (f) geodetic measurements[10].

Nainital Fault and Sleepy Hollow Fault

The Nainital Fault (Figure 2) is a normal fault that divides the deformed synclinal Nainital Massif into two parts. The Naini Peak was uplifted along the Nainital

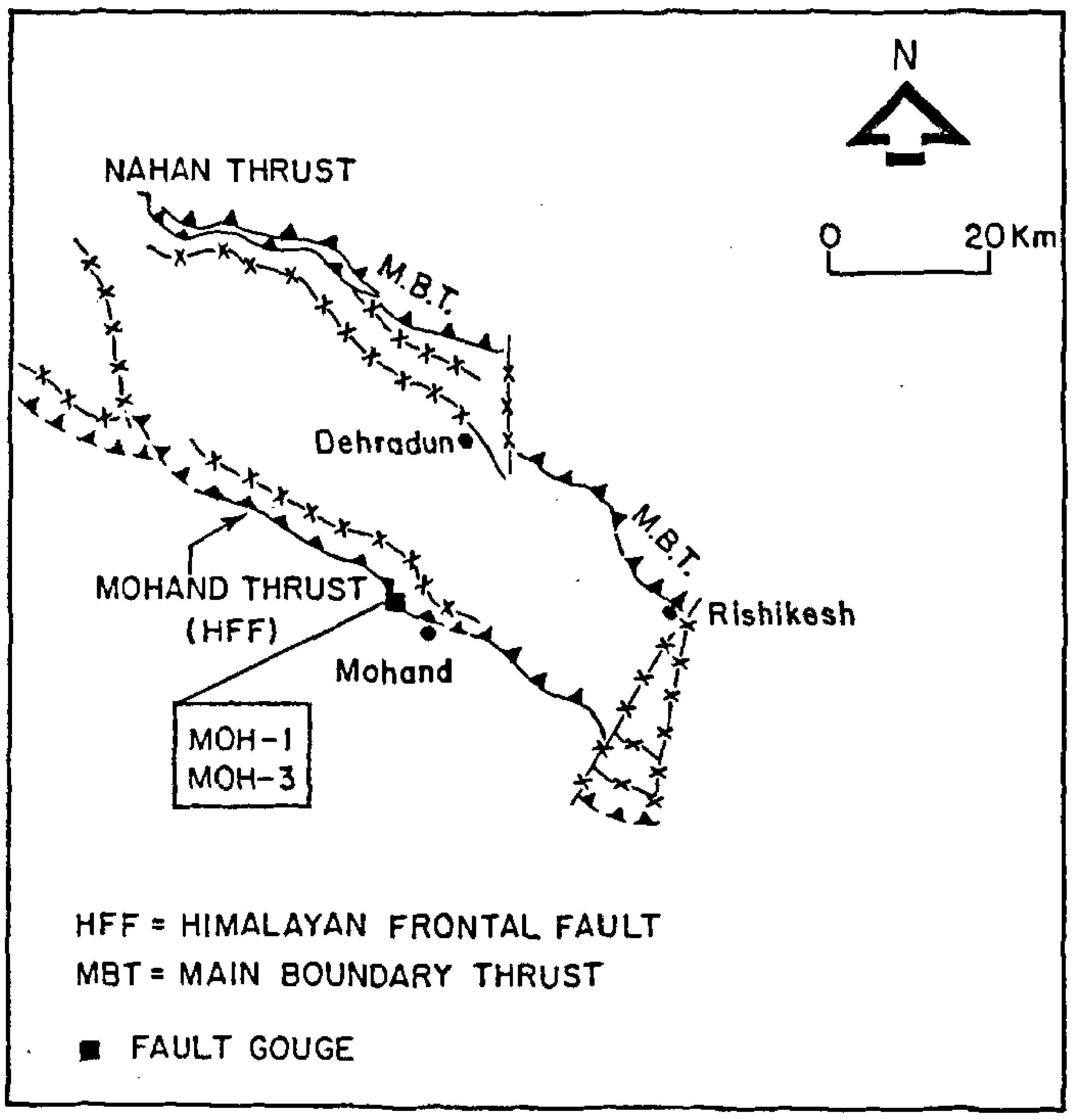

Figure 3. Tectonic map around Dehradun indicating the sampling locations.

Fault relative to the Deopatta Peak in the south[11]. This vertical movement is suggested to be rotational (dip-slip and strike-slip) and caused blocking of a stream, thus forming the Naini Lake[8]. Displacement of river terraces and fans, abandonment of old channels, reversal and blocking of drainage are other indicators of neotectonism[11]. Recent landslides and rockfalls including the 1880 and 1898 events have reduced the dimension of the lake. The Sleepy Hollow Fault is antithetic to the Nainital Fault and is defined by vertical scarps and a straight steep slope demarcating Sleepy Hollow[11].

Mohand Thrust

The Mohand Thrust Zone (Figure 3) is sympathetic to HFF and is located 25 km south of Dehradun. Geodetic measurements at Dehradun show that the Dun Valley is being uplifted at a rate of 1 mm/year[12]. Presence of scarps, slickenslides in the fault zone, displacement and warping of rocks and unpaired terraces indicate neotectonism.

Experimental techniques

The fault gouges were taken from spots approximately 0.5–1 m behind the exposed surface and were pretreated with 1 N HCl (for removing carbonates) and 30% H_2O_2 (for removing the organic fraction). These samples were then subdivided into *coarse* (> 106 μm) and *fine grain fractions* (< 106 μm, from which the 4–11 μm fraction was extracted after deflocculation with 0.01 N Na-oxalate followed by Stokes separation and deposition onto aluminium discs) to conform to the standard luminescence dating analysis procedures[13]. The coarse fraction was dry-sieved for obtaining different grain-size fractions and deposited onto stainless steel discs using Silkospray. Although the 420–500 μm grain size fraction was also sieved for various samples, it could not be used for dating analysis due to significant loss of sample grains during analysis steps. Even small movements (tilting the disc by a few degrees) led to grain loss within a few hours of deposition onto stainless steel discs. This grain loss was probably due to absorption of oil (Silkospray) by the fault gouge grains. For host rocks, a 2 mm layer from the surface was removed by sawing a rock fragment with a water-cooled diamond wheel. This was done because of possible exposure to sunlight of the outer surface. Subsequently, the rock fragment was gently crushed and treated with 1N HCl, 30% H_2O_2 and dry-sieved to obtain the 106–150 μm fraction.

TL analysis was done with the optics channel comprising a Schott UG-11 filter and a Chance Pilkington HA-3 filter coupled to an EMI 9635QA photomultiplier tube and a photon counting system. Fused silica neutral density filters were used for brighter samples. The heating rate used was 2°C/s for coarse fractions and 5°C/s for the fine (4–11 μm) fractions. The 4–11 μm fractions were preheated to 220°C for 1 min. No preheating was done on the coarse grain fractions so as to minimize grain loss. This implied that the width of the age plateau was likely to be smaller as compared to a preheated sample. Laboratory beta irradiations were carried out using a ~1 GBq $^{90}Sr/^{90}Y$ beta source. Alpha irradiations were carried out using a six seater ~0.01 GBq mCi ^{241}Am vacuum alpha irradiation system[14]. Additive dose method was used for estimation of paleodoses. A supralinearity correction was also determined by constructing the second glow growth curve. This correction was added onto the paleodose to obtain the total paleodose. Due to the build-up effect[13], the average dose received by coarser grains is higher than that received by a layer of fine grains (4–11 μm). Multiplicative factors computed for grains of various thicknesses by Wintle and Aitken[15] were used in the present studies. Grain size-dependent attenuation factors provided by Mejdahl[16] were used in estimating the annual dose for the fault gouges. In the dose-rate analysis, thick source ZnS (Ag) alpha counting was used and equal alpha activity of ^{238}U and ^{232}Th series was assumed. Typical errors in alpha count-rates were < 3%. Potassium concentration was determined using NaI(Tl) gamma ray spectrometry. The annual dose included an alpha dose contribution for both fine and coarse grains in view of the fact that the grains originate from a fine-grained shale with uniform spatial distribution of alpha activity.

Zeroing of TL and ESR signals in fault gouges

Zeroing of pre-existing signals – earlier studies

The fundamental assumption in dating fault gouges is that the thermoluminescence signal is completely reset during faulting. For this to happen, basically two types of mechanisms are considered – thermal or shear and hydrostatic pressure/stress effects. In practice, perhaps both effects contribute, but in all the studies (including the present one), the effect of individual processes on the dating signal has been examined.

Thermal effects: It is well known that heat can be generated during faulting and if the temperature exceeds 1000°C, formation of new glassy phases (psuedotachylites) is likely[6,17–19]. Fukuchi *et al.*[20,21] suggested the use of different ESR centres in quartz (OHC, Ge, Al, E′ centres) with different thermal stabilities for zeroing to determine the faulting age. Thermal annealing experiments[21] show that while Al and E′ centres are completely reset above 350°C, OHC and Ge centre are reset only above 400°C. Thus, identical ESR age estimates for different centres with different thermal stability would suggest a complete zeroing of the ESR signals during faulting.

Pressure/stress effects: Ikeya *et al.*[3] suggested that hydrostatic stress could also erase the geological ESR signal during faulting. Experiments using pressures up to 60 MPa, stress and displacements and ring shearing experiments indicated that pressures of a few MPa and displacements of few tens of centimetres can cause an erasure of ESR signals[22–25].

Other experimental data[24] also indicated that the ESR ages for various centres decrease with grain size and attain a stable value below a critical grain size. Recently, Ikeya *et al.*[26] proposed a new isochron method for ESR dating of fault gouge. In this method, the paleodoses obtained for various grain sizes are plotted as a function of external annual dose; the slope of the curve then gives the isochron age.

In the context of Himalaya and the present application of luminescence, studies by Scott and Drever[27] are noteworthy as these indicate the presence of glass which suggest that temperatures during faulting could have reached 1000°C. Experiments by Hase[28] on TL of samples from fault zones suggest that the crushed material had significantly lower luminescence compared to that from the parent rock. Shearing experiments indicated a reduction in TL intensity of quartz grains on the application of normal stress. The above mentioned studies indicate that during faulting, zeroing of luminescence would occur both due to shear stresses and frictional heating. An aspect that merits consideration is the fact that prior to faulting, the sample was buried deeper at a substantially elevated temperature. In the present case, assuming an exhumation rate of 3–5 cm/a, a faulting event 50 ka ago would imply a burial depth in excess of 2–3 km with ambient temperature in the vicinity of 100°C or more. From the TL kinetics point of view, this would imply a two to three order of magnitude lesser thermal stability of the luminescence signal, as compared to lower temperatures near the surface. This implies a higher probability of zeroing.

Zeroing of luminescence – Present work

Based on the foregoing discussion, the following experiments were performed to establish criteria to ascertain that the luminescence of the sample was indeed zeroed during the faulting. These are: (a) variation of paleodose with grain-size, (b) variation of paleodose in a profile transverse to faulting plane, (c) mechanoluminescence characteristics of host rock and fault gouge, and (d) clay mineralogical studies towards estimation of thermal history. It would indeed be desirable to supplement the above mentioned studies with a detailed thin section analysis of the rocks and gouge samples for determination of stress regimes and their effect on the luminescence signal (M. Mukul, pers. commun.).

Grain size dependence of TL ages (Fault gouges)

Previous studies on the variation of ESR ages with grain size have shown that the ESR signals of grains smaller than a certain critical size are zeroed completely[23,24]. Larger grains can retain some relic ESR signal that would result in overestimation. Reflecting upon the differences in thermal conductivity between various grain sizes, it is plausible to expect that resetting of the luminescence signal in smaller grain fractions would occur more readily compared to larger ones. This is because smaller grains achieve a thermal equilibrium earlier. Figures 4 *a*, *b* and Table 1 present the fault gouge TL ages for different grain-size fractions. The results suggest that TL ages attain a constant value (within errors) below a certain critical grain size R_C. It is expected that grains smaller than R_C would have experienced a complete resetting of their TL signal and hence ages based on these should be reliable. In the present study, R_C for fault gouges from the Nainital Fault and Mohand Thrust, was estimated as < 250 μm. For MBT, TL ages for various grain sizes below 420 μm agreed within experimen-

Table 1. Grain-size dependence of luminescence ages

Sample	Location	Grain-size (µm)	Technique	Paleodose (Gy)	Annual dose (mGy/a)	TL age (ka)
KU93-1	Nainital fault	4–11	TL	308 ± 61	7.6	41 ± 7
KU93-1		106–150		224 ± 45	6.5	35 ± 7
KU93-1		212–250		339 ± 20	6.2	55 ± 6
KU93-1		300–420		710 ± 68	6.0	120 ± 15
KU91-4	Nainital fault	106–150	TL	264 ± 39	6.95	38 ± 8
TLV-3*		150–250		290 ± 30	7.0	41 ± 5
TLV-3*		400–420		473 ± 50	6.8	70 ± 9
TLV-1	Main boundary thrust	4–11	TL	542 ± 33	7.9	68 ± 8
TLV-1		106–150		468 ± 65	7.7	61 ± 9
TLV-1		212–250		495 ± 114	7.3	68 ± 13
TLV-1		300–420		571 ± 68	7.1	80 ± 12
MOH-1	Mohand thrust	106–150	IRSL	202 ± 40	4.0	51 ± 9
MOH-1		250–420		258 ± 35	3.1	83 ± 11

*TLV-3 was collected from approximately the same location as KU91-4.

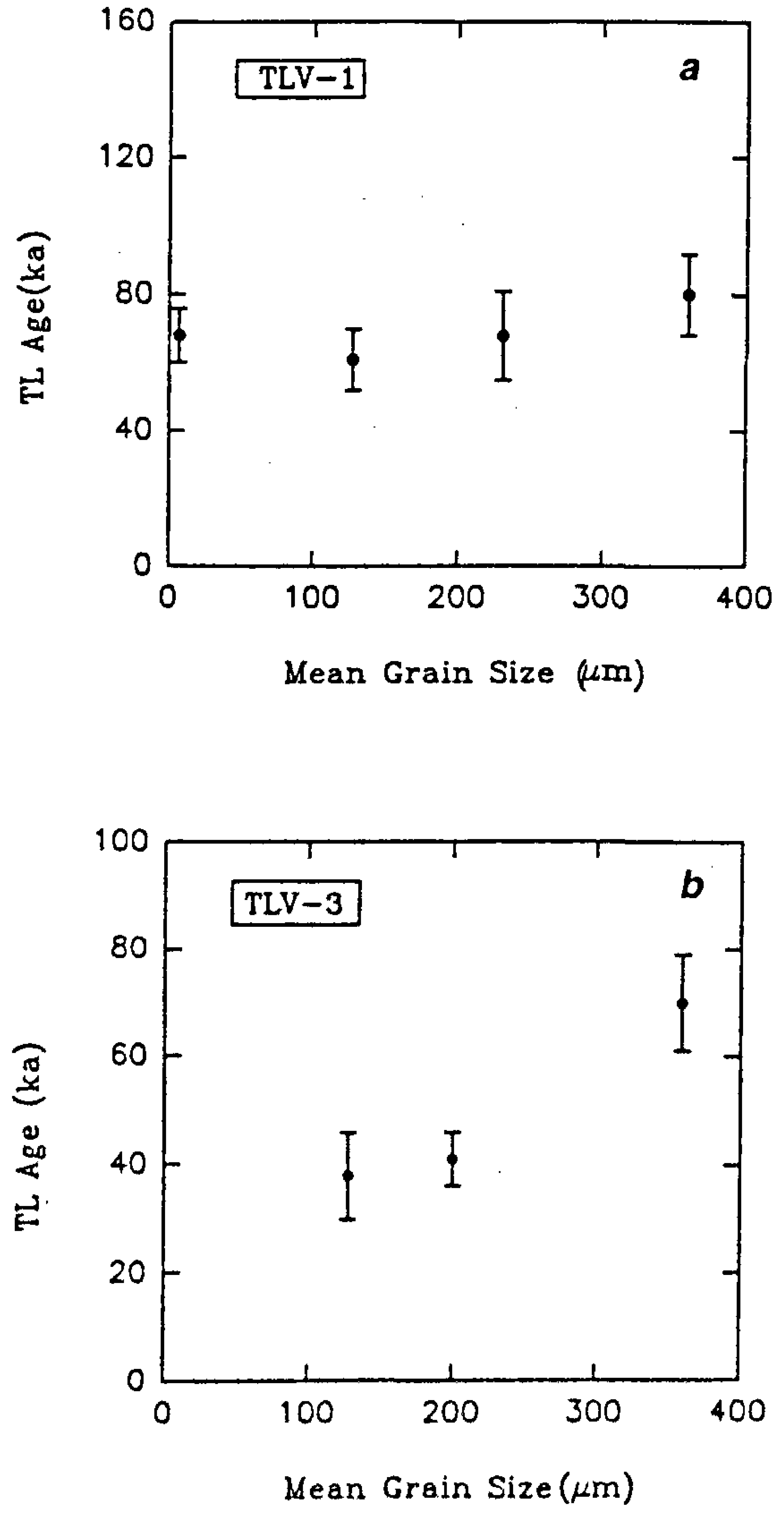

: 4. Variation of TL age with grain-size (*a*) sample TLV-1 and V-3.

tal errors. The data suggest that R_C for MBT is > 420 µm consistent with the concept of bulk heating that may have occurred here. As mentioned above, experimental difficulties precluded TL age estimation on 420–500 µm fraction or higher grain size fractions. These observations can be understood in the following manner. During faulting, the maximum build-up of stress occurs around defects (point defects, dislocations or surfaces) present within grains. These stresses give rise to microcracks that combine to form intra- and inter-grain fractures[7]. When grains impinge upon each other, development of large localized stresses is likely[29]. The fraction of grain volume experiencing such high stresses increases with decreasing grain size (since intra-grain boundaries comprise a small part of the grain volume). So, it is likely that TL signals of smaller grains will be reduced to a greater extent compared to those of larger grains. Since grain boundaries encompass a limited fraction of the grain volume, smaller grains at the boundary would be more efficiently zeroed in comparison to larger ones. Frictional heating while strain energy is being dissipated during faulting provides additional zeroing mechanism[1,24]. This local heating effect is maximum around the grain boundaries where stress concentration is also maximum. Thus, a zone should exist around the grain boundaries where TL signal of the grains is likely to be zeroed completely. This explains the observed grain-size dependence of TL ages.

Bulk heating of the fault gouge has also been proposed as a method of zeroing the ESR/TL signal of fault gouges[29,30]. However, with the exception of MBT fault gouge (TLV-3) in the present case, bulk heating is unlikely to have occurred in other sites. The time-scales of thermal conduction for a spherical grain can be esti-

Table 2. Luminescence dating results for fault gouges and host rocks

Sample	Type	Location	Grain-size (μm)	Technique	Paleodose* (Gy)	Annual dose (mGy/a)	Age (ka)
KU91-4	Fault Gouge	Nainital Fault	106–150	TL, additive dose	264 + 39	16.95	38 + 8
KU91-5	Fault Gouge	Nainital Fault	4–11	TL, additive dose	375 + 30	8.5	44 + 4
KU93-1	Fault Gouge	Nainital Fault	4–11	TL, additive dose	308 + 61	7.6	41 + 7
KU93-2	Distal Fault	Nanital Fault	106–150	TL, additive dose	827 + 141	9.15	90 + 15
KU93-7	Fault Gouge	Sleepy Hollow Fault	106–150	TL, additive dose	311 – 31	8.7	36 + 5
KU93-89	Distal Fault	Sleepy Hollow Fault	106–150	TL, additive dose	518 – 39	6.3	82 + 1
TLV-1	Fault Gouge	Main Boundary Thrust	4–11	TL, additive dose	542 – 33	7.9	68 + 8
TLV-3	Fault Gouge	Nainital Fault	150–250	TL, additive dose	290 + 30	7.0	41 + 5
TLV-5	Fault Gouge	Main Boundary Thrust	106–150	TL, additive dose	102 + 17	1.4	72 + 12
KU93-5	Host Rock	Sleepy Hollow Fault	106–150	TL, additive dose	≥ 850 + 255	–	–
KU93-6	Host Rock	Sleepy Hollow Fault	106–150	TL, additive dose	≥ 650 + 128	–	–
MOH-1	Fault Gouge	Mohand Thrust (HFF)	106–150	IRSL, additive dose	202 + 40	4.0	51 + 9
MOH-3	Fault Gouge	Mohand Thrust	106–150	TL, additive dose	316 + 44	4.9	64 + 9
MOH-3	Fault Gouge	Mohand Thrust	106–150	IRSL, additive dose	310 + 26	4.9	63 + 7.4

*Includes supralinearity correction; HFF = Himalayan Frontal Fault.
The mean of fault gouge TL ages from the Main Boundary Thrust is 70 ka.
The mean of fault gouge TL ages from the Nainital Fault is ~41 ka.
The mean luminescence age of fault gouges from the Mohand Thrust is ~59 ka.

mated using the expression,

$$K\nabla^2 T = \delta T/\delta t;\ \tau = a^2/K\pi^2,$$

where a is a dimensional parameter, K the thermal diffusivity, and τ the characteristic time (in seconds) for heat conduction[31]. Thus, using a typical value of 10^{-6} m^2/s for thermal diffusivity K, the characteristic time is $10^5 a^2$. The characteristic time of heat conduction for 1000 μm and 100 μm grains is 0.1 s and 10^{-3} s respectively. Thus, grains of size 1000 μm are expected to be in thermal equilibrium with 100 μm grains in 0.1 s. This implies that if bulk heating is responsible for zeroing of TL signals, 300–400 μm TL age should be identical to TL ages for size ranges < 300 μm within experimental errors. The critical grain size value for MBT fault gouges is greater than Nainital Fault and Mohand Thrust fault gouges. This is probably due to availability of greater stress energy and larger displacement during faulting at the MBT. This is a reasonable assumption considering that MBT is the major fault system in this region. Movements along MBT and MCT have been suggested to be greater and faster since the frontal ranges related to them have acquired greater heights and ruggedness[9]. Other possibilities are that bulk heating may have occurred in MBT, and thus a critical grain size may not exist for the MBT fault gouge sample; a ductile deformation history may also explain such an occurrence.

Fault gouge paleodoses

Table 2 provides the estimate of paleodoses from the host rock and fault gouges. The paleodoses (200–500 Gy, see Table 2) for fault gouges are appreciably smaller in comparison to host rock paleodoses of > 650–850 Gy. The concordance of fault gouge ages (41 ± 5 ka, 41 ± 7 and 44 ± 4 ka) on samples derived from rocks of different age and depositional environment indicates that a definite TL resetting event is being seen. Additionally, TL intensities of host rocks a few meters away from fault zones, are up to two orders of magnitude higher compared to fault gouges, suggesting that near complete resetting of the geological TL signal occurred during faulting.

Mechanoluminescence studies

Luminescence induced during mechanical deformation of solids is called mechanoluminescence (ML). Various materials such as organic and inorganic crystals, amorphous solids, glasses, and minerals exhibit mechanoluminescence. Most of these materials emit ML during their fracture, but some (e.g. coloured alkali halides, alkaline earth oxides and some rubbers) exhibit ML in their elastic and plastic regions. In X-ray or gamma ray-irradiated alkali halide crystals, ML excitation takes place during dislocation movement. In the dislocation annihilation model, annihilation of dislocations of opposite sign may produce a high temperature locally, which results in luminescence emission as in thermoluminescence[32]. Since the zeroing of the TL signal can occur due to development of stresses during faulting, it was considered that ascertaining the dependence of ML of fault gouges with applied pressure could provide a useful complement to the present studies. For ML studies, sieved fault gouges and host rocks samples were mechanically deformed and the ML intensity was measured using the experimental set which permitted 800 g weight to be dropped from different heights for striking the sample at different impact velocities and therefore at different applied pressures. The sample was placed on a transparent lucite plate inside a sample holder below the guiding cylinder. An RCA 931A photomultiplier tube placed below the transparent lucite plate and connected to a phosphorescent screen oscilloscope was used for measuring luminescence. Response time of PMT of 5 μs was adequate to measure ML pulses of a few milliseconds duration. For ML measurements, the sample was wrapped in thin aluminium foil and fixed on lucite plate with an adhesive tape. Lucite does not emit any luminescence under application of pressure and the aluminium foil reflected light and ensured that the sample fragments did not disperse when impacted by the load. ML at different applied pressures was recorded by tracing the ML pulse appearing on the oscilloscope screen. The impact velocity was estimated as $(2gh)^{1/2}$, where g is the acceleration due to gravity and h the distance of fall. The applied pressure σ is then computed using the expression

$$\sigma = M\sqrt{(2gh)}/t_c A,$$

where M is the mass of load, A the area of sample and t_c the interaction time. This method for estimating applied pressure is only an approximate one, and thus the pressure estimates are not absolute. The width of the ML pulse (typically 0.4–0.6 ms) was assumed to be the interaction time. Figures 5 *a, b* show the dependence of ML intensity on applied stress for a typical fault gouge (TLV-3) and host rock (TLV-2) sample respectively. The ML intensities of host rocks are up to five times higher in comparison to fault gouges. It was also observed that if the mass was repeatedly dropped onto the host rocks and fault gouges, ML emission was observed during the first two/three impacts. Subsequent impacts did not give rise to ML emission. These observations suggest that (a) host rocks luminescence have not been recently reset and (b) energy stored as ML in host rocks and fault gouges gets liberated during faulting. Thus, repeated impacts reduce ML emission. The minimum pressure required to initiate ML emission from host rocks and fault gouges was estimated to be 200 MPa. The strength of the upper crustal rocks is also of the same order[7]. Thus, it is probable that seismic events of magnitudes > 6 will release energy from host rocks as ML. It is suggested that a comparative study of ML from host rock and fault gouge can provide some indication of release of ML energy during the formation of fault gouge. Further, there is a case to study the dependence of ML growth and effect of impacts on TL of the samples and these aspects will be pursued in future.

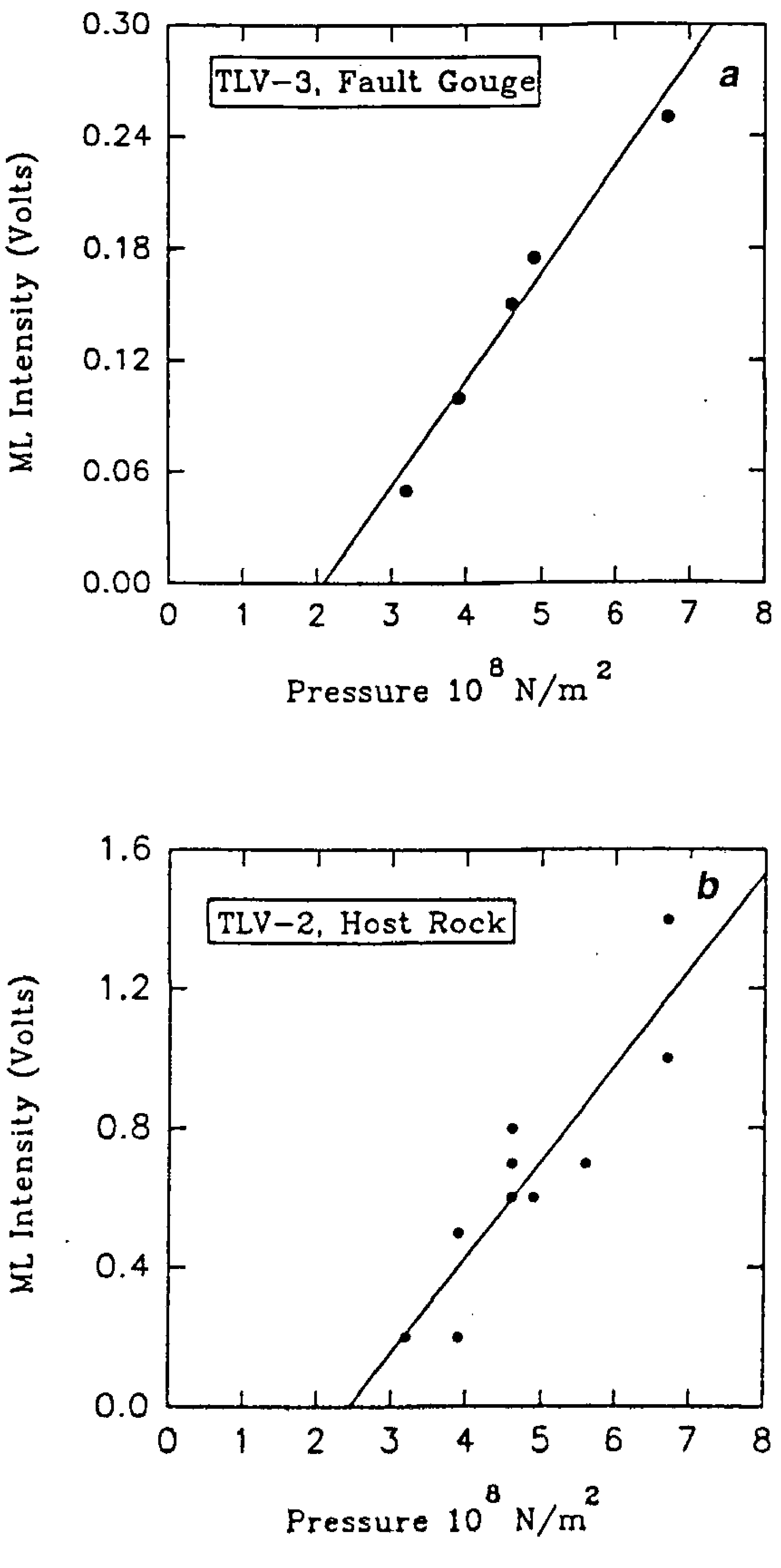

Figure 5. Variation of mechanoluminscence intensity vs applied pressure: (*a*) Fault gouge, (*b*) Host rock.

Clay-mineralogical studies

Illite

Structures of minerals illite and chlorite undergo changes on heating. It was thus considered that changes in structural parameters of these minerals could be used to assess thermal excursion during faulting. The basic premise in this study was illite crystallinity which is estimated by a parameter that measures the nature of 10 Å (001), XRD (X-ray diffraction) peak. On heating, illite loses interlayer water and adsorbs potassium. A rearrangement of ions occurs as potassium gets fixed in the interlayer positions. This phenomenon manifests itself in increasing sharpness of the 10 Å XRD peak. Weaver[33] first used this increase in sharpness as a measure of low-grade metamorphism. Weber[34] devised a new crystallinity index, the Weber index, expressed as

Table 3. Illite Hb_{rel} values for fault gouges and host rocks

Sample	Type	Location	Illite Hb_{rel}	Inferred thermal excursion
KU91-4	Fault Gouge	Nainital Fault	134	>370°C
KU91-5	Fault Gouge	Nainital Fault	144	>370°C
KU93-1	Fault Gouge	Nainital Fault	155	200–370°C
KU93-3	Host Rock	Nainital Fault	155	200–370°C
KU93-7	Fault Gouge	Sleepy Hollow Fault	124	> 370°C
KU93-8	Rocky Material	Sleepy Hollow Fault	181	200–370°C
S–I	Host Rock	Nainital Fault	120	>370°C
K–I	Host Rock	Nainital Fault	120	>370°C

Table 4. Chlorite peak area ratios and inferred thermal excursions for fault gouges and host rocks

Sample	Type	Location	Chlorite⁺ peak ratio	Inferred thermal excursion
KU91-4	Fault Gouge	Nainital Fault	2.0	< 400°C
KU91-5	Fault Gouge	Nainital Fault	1.5	< 400°C
KU93-1	Fault Gouge	Nainital Fault	1.6	< 400°C
KU93-2	Rocky Material	Nainital Fault	2.0	< 400°C
KU93-3	Host Rock	Nainital Fault	2.0	< 400°C
KU93-4	Host Rock	Nainital Fault	0.8	> 400°C
KU93-6	Host Rock	Sleepy Hollow Fault	0.6	> 400°C
KU93-7	Fault Gouge	Sleepy Hollow Fault	0.8	> 400°C
KU93-8	Rocky Material	Sleepy Hollow Fault	1.9	< 400°C
S–I	Host Rock	Nainital Fault	1.7	< 400°C
K–I	Host Rock	Nainital Fault	1.7	< 400°C
TLV-1	Fault Gouge	Main Boundary Thrust	0.5	> 400°C
TLV-3	Fault Gouge	Nainital Fault	2.2	< 400°C
TLV-5	Fault Gouge	Main Boundary Thrust	0.6	> 400°C
TLV-6	River Terrace Deposit	Nr. Kaladhungi	0.7	> 400°C
CNF-2	Aeolian Sands	Ghaggar Flood Plain	0.5	> 400°C
CNF-9	Alluvial Sands	Chautang Flood Plain	0.3	> 400°C

⁺Ratio of the chlorite 7.1 Å and 14.2 Å peak areas.

$$Hb_{rel} = [Hb\ (10\ \text{Å})_{illite}]/[Hb\ (4\ \text{Å})_{quartz}] \cdot 100,$$

where Hb stands for half peak width. Quartz, being unaffected by heating is used as a standard for interlaboratory comparisons of the Hb_{rel} values. In the present study, Blenkinsop's[35] recommendation on the use of Hb_{rel} values of 149 and 378 as, upper and lower bounds of anchizone (200–370°C) boundary were used to infer the thermal excursion seen by the samples. The illite Weber index was also used to determine the heating temperature of fault gouges and host rocks.

Chlorite peak ratios

Gogte (pers. commun.) has demonstrated previously that the X-ray diffraction patterns of chlorite-bearing clays exhibited a change in the ratio of the peak-areas of peaks at 7.1 Å and 14.2 Å with heating. For temperatures between 0–250°C and 250 ± 400°C, the ratios were 1.6 ± 0.2 and 2.0 ± 0.1 respectively. Between 400 and 500°C, the ratio sharply approached zero. Minerals of the chlorite facies are transformed into chlorite schists and sericite at these temperatures[36]. The chlorite peak ratio method was also used to estimate the faulting temperature. For these studies, sieved grain-size fractions after chemical pretreatment were powdered and placed on a glass slide. XRD measurements were made using a Rigaku D Max II VC XRD system operated at 50 kV, 25 mA, at a scan speed of 1'/s. The intensity, *d*-value, half peak widths and peak areas were computed using standard software packages. The measurements were performed on host rocks, fault gouges, aeolian deposits and alluvium. The latter two types were included to examine the robustness of this approach. Tables 3 and 4 represent the illite Hb_{rel} values and chlorite peak area ratios for the various samples. All samples contain illite, chlorite and quartz. Some samples (TLV-3, TLV-2, etc.) also contained dolomite. The illite Hb_{rel} values indicate that both fault gouges and host rocks were heated beyond 200°C.

Errors associated with chlorite peak ratios are to be taken as underestimates due to exclusion of errors arising from (a) aliquot to aliquot variations and (b) the calculation of peak areas. The suggested peak ratios (based on estimation of chlorite peaks for a minimum of 4 aliquots and repeated calculation of peak areas) are 1.6 ± 0.7 and 0 ± 0.7 for the temperature ranges 0–400°C and > 400°C, respectively. Thus, presently, the peak ratio method can only indicate if a sample is heated above/below 400°C. The chlorite peak ratios (Table 4) indicate that besides fault gouges, host rocks, alluvium and aeolian deposits were also heated beyond 250°C. This result is puzzling since host rocks or sedimentary deposits should not depict any heating signatures. This apparent discordance perhaps arises due to the fact that illites and chlorites examined from various samples were derived from a common metamorphic provenance. Further, an additional complication could have arisen due to masking of the 10 Å illite and 7 Å chlorite peaks by the 10 Å muscovite and the 7 Å kaolinite peaks. It thus appears that for the present set of rocks and fault gouge samples, the mineralogical studies cannot unequivocally establish if the heating event corresponds to recent faulting/earlier metamorphic events. More research on this aspect is necessary and may be rewarding.

Other studies

Stability of the TL signal – Kinetic parameters

To establish that TL signals of the minerals constituting the sample remain stable over time scales of interest, the trap parameters and mean lives for host rocks and fault gouges were estimated. Lifetime of charges in a particular trap of depth E and frequency factor s at the storage temperature T is expressed as

$$\tau = s^{-1}\exp(E/kT).$$

It can be shown that for any kinetic order, the initial portion of a TL glow curve can be approximated by the relation,

$$\ln I = \text{const.}\ (-E/kT),$$

where I is the TL intensity. Thus a plot of $\ln(I)$ is plotted as a function of $1/kT$, the slope gives the value of the activation energy E. This method, termed as the initial-rise method, can be applied to overlapping peaks using *the fractional glow technique*[37]. *Representative samples* of fault gouges and host rocks were used to determine their activation energy values. The fractional glow technique was utilized on the 106–150 µm fraction of the samples. The samples were directly placed on the heater plate to ensure a better heat conduction and precise temperature measurements. Several 10°C incremental cycles of heating and cooling were performed in

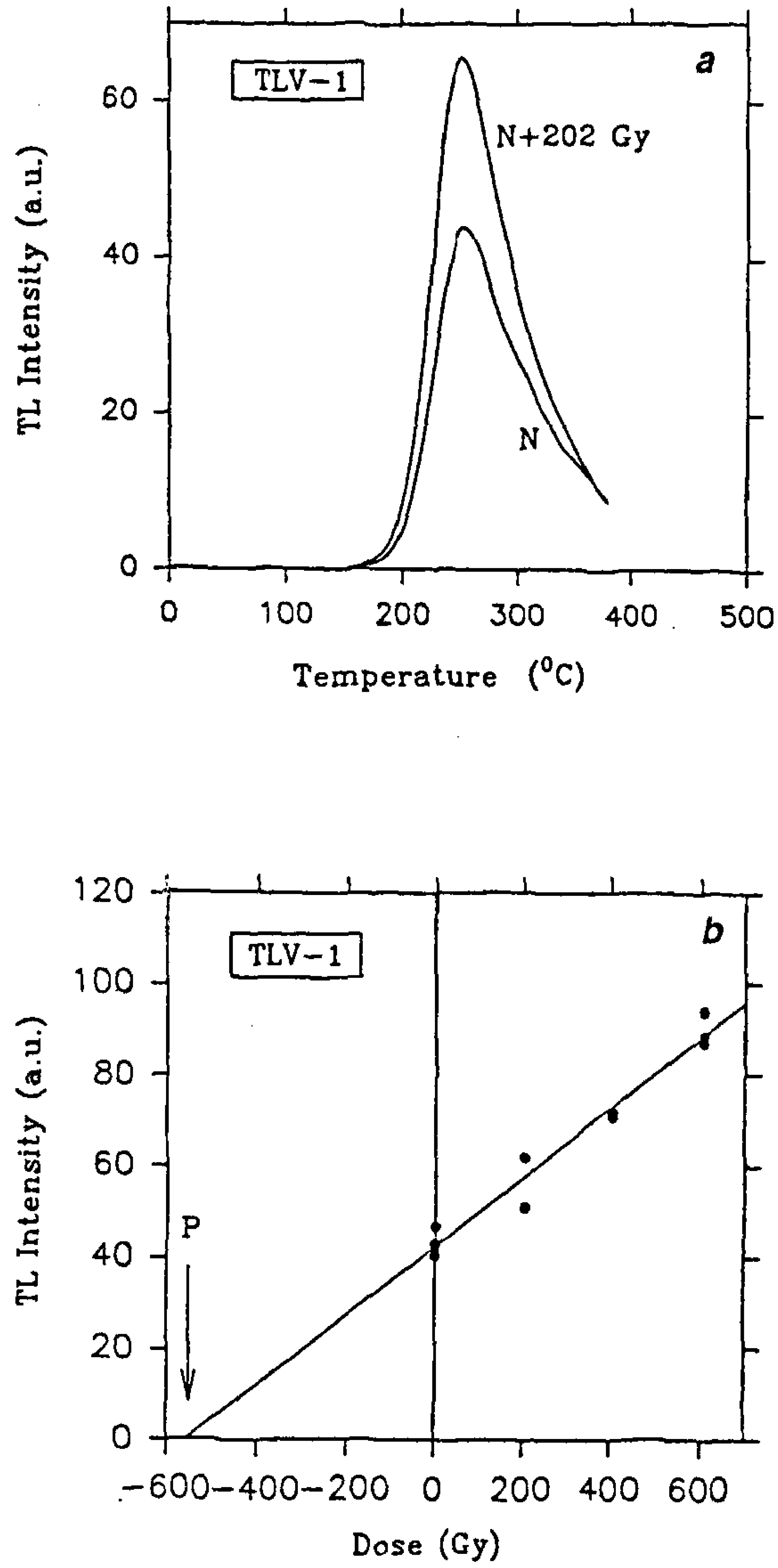

Figure 6. Typical TL glow and growth curve for sample TLV-1.

the temperature range from 200 to 380°C. Figures 6 and 7 represent typical plots of ln (intensity) versus $1/T$ for fault gouges. The dependence of E values on temperature is also shown in Figure 8. Table 5 presents the trap parameters evaluated for the fault gouges and host rocks. The spectra of activation energies for fault gouges determined using the initial rise method are 1.37 eV (210°C) to 1.71 eV (350°C). For the host rock from Sleepy Hollow Fault, the E values ranged between 1.61 eV and 1.67 eV for 310°C and 350°C, respectively. *These values closely correspond to E values of quartz* and K-feldspar as quoted in the literature[13]. The activation energy values were used to calculate the lifetime of the TL signal (at 15°C) assuming first-order kinetics and frequency factors taken from Aitken[13]. Since thermal quenching can additionally affect E values determined using the initial rise method[38], the computed lifetimes are minimum estimates. The lifetimes indicate that TL

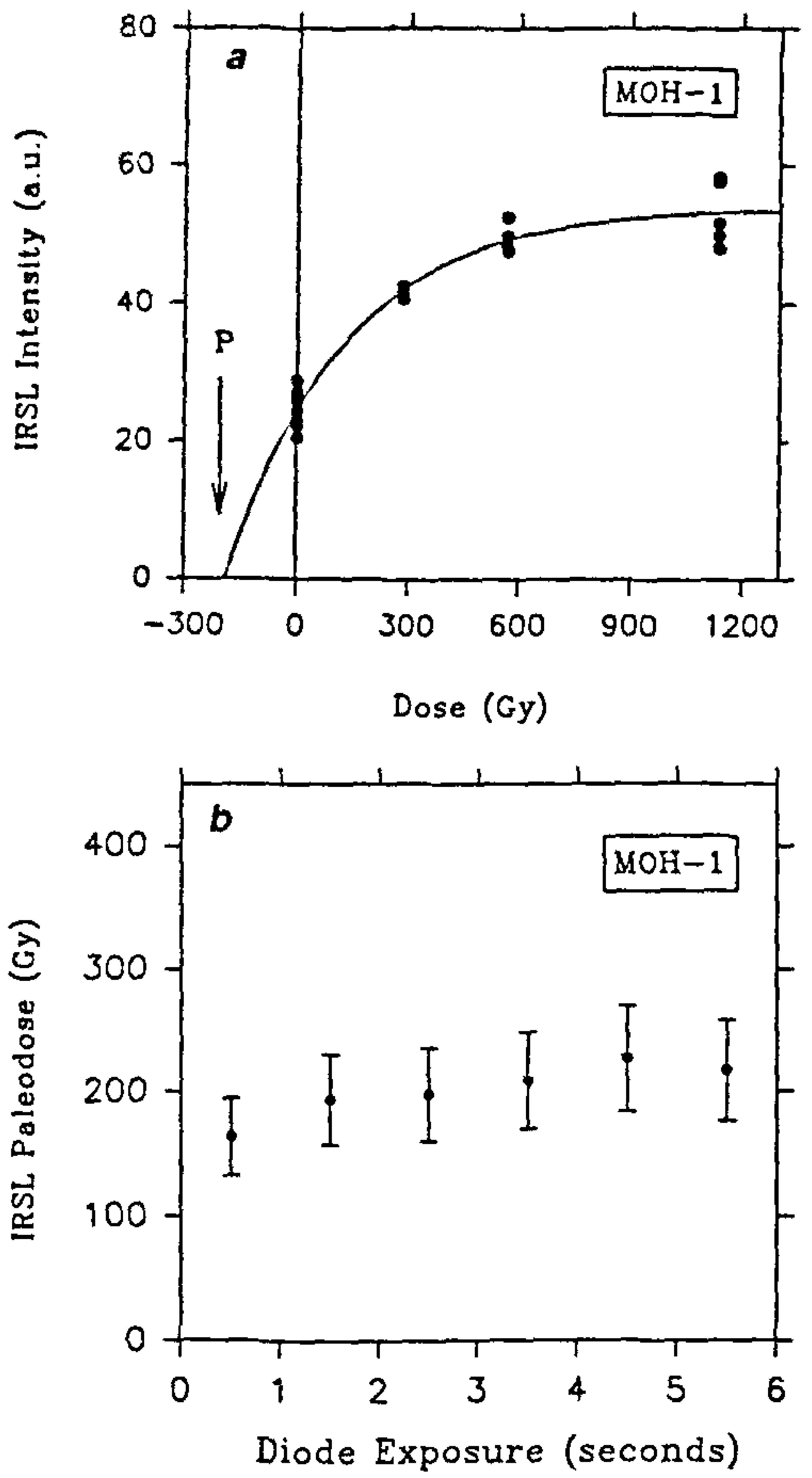

Figure 7. Typical IRSL growth curve and IRSL shine plateau for sample MOH-1.

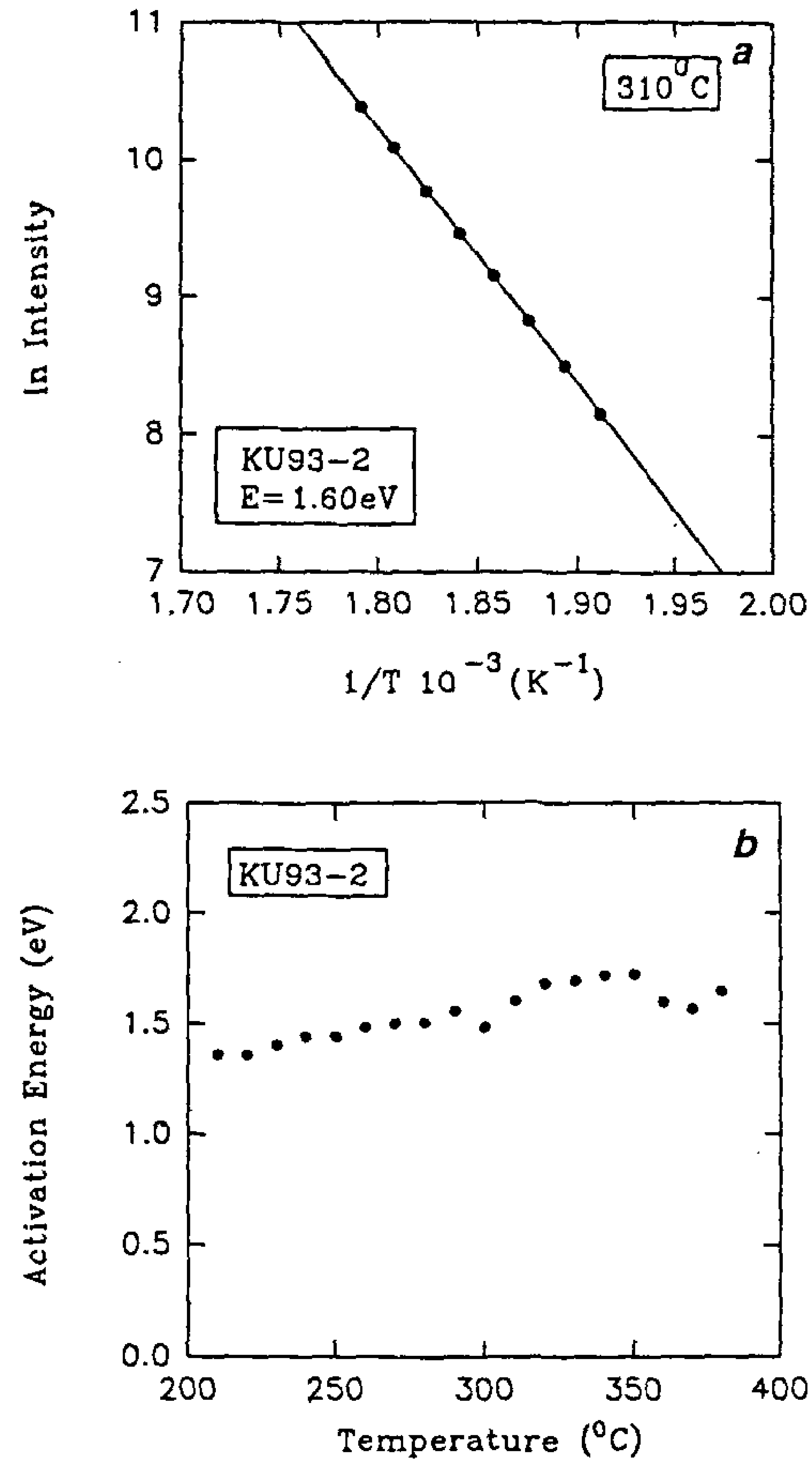

Figure 8. Calculation of activation energy of TL signal from fault gouge sample KU93-1. (*a*) Plot of logarithm of TL intensity vs the glow curve temperature and, (*b*) plot of activation energy vs glow curve temperature.

signal from the 250 to 400°C region of the glow curve is stable over timescales of a million years.

Anomalous fading

Loss of luminescence from the high temperature (> 250°C) stable region of the glow curve is termed 'anomalous fading'. Wintle[38] first reported anomalous fading for various types of feldspars from volcanic lava flows. Luminescence ages affected by anomalous fading are underestimates of the true age. In the present studies, the fault gouges were imparted a beta dose of 340 Gy and subsequently stored for a period of three weeks at 23°C after irradiation. No fading of the TL signal was observed from 250 to 400°C region of the glow curve.

Results – Luminescence ages

Figure 6 provides a typical TL glow curve and growth curve for fault gouges. Figure 7 provides IRSL growth curve and shine plateau for a fault gouge. Tables 2 and 6 present radioactivity data and luminescence ages of fault gouges and host rocks. Radioactivity data indicate that the annual dose from fault gouge from Nainital and its vicinity is 4–9 mGy/a. The annual dose from TLV-5 from Bajyun, MBT is 1.4 mGy/a, due perhaps to a dilution by limestone carbonates. In general, the radioactivity concentration of fault gouges is high as the fault zones often serve as sites of mineralization (K. S. Valdiya, pers. commun.).

Aliquot-to-aliquot scatter in TL intensity for coarse-grained fractions was generally higher than the 4–11 μm fraction. IRSL dating was also performed along with TL dating on Mohand Thrust fault gouges. IRSL (63 ± 7 ka) and TL ages (64 ± 9 ka) along Mohand Thrust concur within experimental errors. This also suggests that IRSL dating can be developed for dating of heated objects. Since TL intensities from host rock samples exhibited a saturating behaviour over a large range of applied dose 0–800 Gy, the host rock paleodoses are minimum estimates and have a large error associated with them.

Table 5. Activation energies, frequency factors and lifetimes for fault gouges and host rocks

Sample	Glow curve temp (°C)	Activation energy (eV)	Activation energy (eV)	Frequency* factor (s^{-1})	Lifetime# (years at 15°C)
KU93-1	210	1.37	1.40	28×10^{13}	$\sim 0.7 \times 10^3$
(Nainital Fault Gouge)	280	1.56	1.62	4.1×10^{13}	$\sim 1 \times 10^6$
	310	1.67	1.68	1.8×10^{13}	$\sim 200 \times 10^6$
	320	1.60	1.60	1×10^{13}	$\sim 20 \times 10^6$
	350	1.71	1.68	2.8×10^{12}	$\sim 6 \times 10^9$
KU93-2	210	1.36	1.40	2.8×10^{13}	$\sim 0.5 \times 10^3$
(Nainital Fault Gouge)	310	1.60	1.60	1×10^{13}	$\sim 20 \times 10^6$
	320	1.68	1.69	1×10^{14}	$\sim 50 \times 10^6$
	350	1.72	1.68	2.8×10^{12}	$\sim 9 \times 10^9$
	380	1.65	1.66	1.5×10^{13}	$\sim 100 \times 10^6$
KU93-5	310	1.61	1.68	1.8×10^{13}	$\sim 20 \times 10^6$
(Sleepy Hollow Host Rock)	320	1.55	1.60	1×10^{13}	$\sim 3 \times 10^6$
	330	1.69	1.69	1×10^{14}	$\sim 80 \times 10^6$
	350	1.67	1.68	2.8×10^{12}	$\sim 1 \times 10^9$
KU93-7	220	1.36	1.40	2.8×10^{13}	$\sim 0.5 \times 10^3$
(Sleepy Hollow Fault Gouge)	320	1.57	1.60	1×10^{13}	$\sim 6 \times 10^6$
TLV-3	210	1.45	1.40	2.8×10^{13}	$\sim 20 \times 10^3$
(MBT Fault Gouge)	320	1.55	1.60	1×10^{13}	$\sim 3 \times 10^6$
	370	1.61	1.66	1.5×10^{13}	$\sim 2 \times 10^7$

*At a glow-curve temperature T°C, the estimated sample activation energy was compared with activation energy for minerals (at ~T°C) quoted in Aitken[13]. The frequency factor for the activation energy nearest to the sample activation energy at ~ T°C was assumed to be the sample's frequency factor(s).

#Lifetimes have been calculated using sample activation energy (column 3) and *s* values (frequency factor) (column 5) assuming a first-order kinetics.

Table 6. Radioactivity data for fault gouges and host rocks

Sample	Type	Th* (μg/g)	U (μg/s)	K+(%)	Annual dose** (mGy/a)
KU91-4	Fault Gouge	12.4	5.1	3.0	6.95
KU91-5	Fault Gouge	11.7	6.2	4.0	8.5
KU93-1	Fault Gouge	13.6	3.9	3.7	7.6
KU93-2	Rocky Material	21.3	6.2	4.7	9.15
KU93-7	Fault Gouge	18.6	5.4	4.9	8.7
KU93-8	Rocky Material	12.7	3.7	3.7	6.3
TLV-1	Fault Gouge	18.5	5.4	3.7	7.9
TLV-3	Fault Gouge	20.7	6.1	2.7	7.0
TLV-5	Fault Gouge	2.4	0.7	0.85	1.4
MOH-1	Fault Gouge	9.1	2.6	1.3	4.0
MOH-3	Fault Gouge	12.3	3.6	1.2	4.9

*Error in Th and U concentrations is typically ~10%.
**Water content (assumed) = 20% ± 6%.
+Error in *K* concentration is typically ~5%.

The samples KU91-4 and TLV-3 were collected near Jeolikot, and KU91-5 and KU93-1 were collected near Deopatta, Nainital Fault. The TL ages for these fault gouges (Table 2) indicate that TL ages are reproducible. This also suggests complete resetting of the luminescence signal. Such concordance is unlikely to occur otherwise.

The luminescence dating results provide evidence for neotectonic activity at the Nainital and Sleepy Hollow Fault at 41 ± 8 ka and 36 ± 5 ka respectively. The Mohand Thrust fault gouge is dated to 59 ± 10 ka. Fault gouge in MBT gave an age of 70 ± 12 ka. There are no other age estimates and hence a direct validation or otherwise of luminescence ages is not possible. However, radiocarbon analysis of lake sediments from lakes contemporary to Nainital Lake gives a ~50 ka formation age of Nainital Lake which is believed to have been created by tectonic movement along Nainital Fault. Along the North Almora Thrust and South Almora Thrusts (30 km from Nainital), faulting resulted in the blocking of rivers and formation of lakes[39]. ^{14}C dating of charcoal from Naukuchyatal-Bhimtal (30 km from Nainital) indicates that this was formed 44 ka BP by movements along Kotli Fault, which runs parallel to North Almora Thrust[37]. Thus, the agreement between formation age of Nainital Lake and other lakes including Lake Wadda and the TL faulting age lends credence to the applicability of the luminescence dating techniques. Luminescence dating of soft sediment deformation structures from Spiti Valley, Himachal indicated that large paleoearthquakes took place in Spiti valley at 90 ka, 61 ka, 37 ka and 26 ka (ref. 38). A correlation between these ages and luminescence ages of faulting in Nainital and Mohand suggests the possibility of regionally extended tectonism in Himalaya at ~40 ka and at ~60 ka. Samples (KU93-2 and KU93-8) collected ~3–4 m away from fault gouges gave higher TL ages (90 ± 15 ka, 82 ± 10 ka) compared to ages obtained at the fault. This is probably a consequence of (a) partial zeroing of the TL signal during faulting at 40 ka or, (b) an older faulting event (possibly contemporaneous with the 70 ± 12 ka MBT event at 86 ka since the possibility of repeated faulting events in the same zone cannot be ruled out). Scholz has demonstrated that recurrence of faulting (increasing slip) results in increasing thickness of the gouge zone produced during faulting. Further dating work is necessary to resolve this issue.

Summary

(a) Absolute dating of fault gouges using thermoluminescence and IRSL technique has been attempted for the first time. The basic approach was to examine the possibility of developing criteria that could provide independent evidence for zeroing of the fault gouge TL signal. Present experimental data indicates that grains smaller than a certain threshold size have their TL signals completely reset during faulting.

(b) TL ages on fault gouges imply that tectonic activity took place along Nainital Fault and Sleepy Hollow Fault at 41 ± 8 ka and 36 ± 5 ka respectively. The Main Boundary Thrust and the Mohand Thrust were tectonically active at 70 ± 12 ka and 58 ± 10 ka respectively.

(c) Luminescence ages of fault gouges from Nainital, Mohand and seismites from Spiti provide a first chronometric evidence of regionally extended tectonism in the Himalaya around 40 ka and 60 ka.

1. Singhvi, A. K., Banerjee, D., Pande, K., Gogte, K. and Valdiya, K. S., *Quat. Geochron.*, 1994, **13**, 595–600.
2. Banerjee, D., Ph D Thesis (unpubl.) 1997, Gujarat University, Gujarat.
3. Ikeya, M., Miki, T. and Tanaka, K., *Science*, 1982, **215**, 1392–1393.
4. Forman, S. L., Machette, M. N., Jackson, M. E. and Maat, P., *J. Geophys. Res.*, 1989, **94(B2)**, 1622–1630.
5. Forman, S. L., Nelson, A. R. and McCalpin, J. P., *J. Geophys. Res.*, 1991, **96(B1)**, 595–605.
6. Sibson, R. K., *Geophys. J. R. Astron. Soc.*, 1975, **43**, 775–794.
7. Scholz, C. H., *The Mechanics of Earthquakes and Faulting*, Cambridge University Press, New York, 1990, p. 439.
8. Valdiya, K. S., in *Zagros-Hindukush-Himalaya: Geodynamic Evolution* (eds Gupta, H. K. and Delany, F. M.), American Geophysical Union, 1981, pp. 87–110.
9. Valdiya, K. S., *Ann. Tecton.*, 1992, **6**, 54–84.
10. Ansari, A. R., Chugh, R. S., Sinvhal, H., Khattri, K. N. and Gaur, V. K., *Himal. Geol.*, 1976, **49**, 323–337.
11. Valdiya, K. S., *Geology and Natural Environment of Nainital Hills*, Gyanodaya Prakashan, Nainital, 1988, p. 155.
12. Rajal, B. S., Virdi, N. S. and Hasija, N. L., Survey of India, 1986, pp. 146–159.
13. Aitken, M. J., *Thermoluminescence Dating*, Academic Press, London, 1985, p. 359.
14. Singhvi, A. K. and Aitken, M. J., *Ancient TL*, 1978, **3**, 2–9.
15. Wintle, A. G. and Aitken, M. J., *Int. J. Radiat. Isotopes*, **28**, 625–627.
16. Mejdahl, V., *Quat. Sci. Rev.*, 1988, **7**, 347–348.
17. McKenzie, D. and Brune, J. N., *Geophys. J. R. Astron. Soc.*, 1972, **29**, 65–78.
18. Tuefel, L. W. and Logan, J. M., *Pure Appl. Geophys.*, 1978, **116**, 840–865.
19. Sibson, R. H., *J. Geol. Soc. London*, 1977, **133**, 191–213.
20. Fukuchi, T., Imai, N. and Shimokawa, K., in *ESR Dating and Dosimetry* (eds Ikeya, M. and Miki, T.), 1985, pp. 211–218.
21. Fukuchi, T., Imai, N. and Shimokawa, K., *Earth Planet. Sci. Lett.*, 1986, **78**, 121–128.
22. Ariyama, T., in *Ionics* (eds Ikeya, M. and Miki, T.), Tokyo, 1985, pp. 249–256.
23. Buhay, W. M., Schwarz, H. P. and Grun, R., *Quat. Sci. Rev.*, 1988, **7**, 515–522.
24. Lee, H. K. and Schwarz, H. P., *Tectonophysics*, 1994, **235**, 317–337.
25. Tanaka, K., Ph D Thesis, University of Kyushu, Japan, 1990, p. 111.
26. Ikeya, M., Tani, A. and Yamanaka, C., *Jpn. J. Appl. Phys.*, **34**, 334–338.
27. Scott, J. S. and Drever, H. I., *Proc. R. Soc. Edin.*, 1953, **65B2**, 121–141.
28. Hase, E., in *Fiscal Meeting of Seismological Society of Japan*, 1983, p. 213.
29. Karnz, R. L., *Tectonophysics*, 1983, **100**, 449–480.
30. Fukuchi, T., *Earth Planet. Sci. Lett.*, 1989, **94**, 109–122.
31. Fukuchi, T., *J. Geol. Soc. London*, 1992, **149**, 265–272.
32. Chandra, B. P., *Nucl. Tracks*, 1985, **10**, 225–241.
33. Weaver, C. E., *Bull. Am. Assoc. Petrol. Geol.*, 1960, **44**, 1505–1518.
34. Weber, K., *Neues Jahrbuch fur Mineralogie Monatshefte*, 1972, **6**, 267–276.
35. Blenkinsop, T. G., *J. Metamorphic Petrol.*, 1988, **6**, 623–636.
36. Dunoyer de Segonzac, *Sedimentology*, 1970, **15**, 281–346.
37. Gobrecht, H. and Hofmann, D. J., *J. Phys. Chem. Sol.*, 1996, **27**, 509–522.
38. Wintle, A. G., *Geophys. J. R. Astron. Soc.*, 1975, **41**, 107–113.
39. Valdiya, K. S., Kotlia, B. S., Pant, P. D., Shah, M., Mungali, N., Tewari, S., Sah, N. and Upreti, M., *Curr. Sci.*, 1996, **70**, 157–162.

ACKNOWLEDGEMENTS. Mechanoluminescence studies were performed at the Department of Physics, R. D. University, Jabalpur and XRD measurements at the Deccan College, Pune. We are grateful to Prof. K. S. Valdiya for help and guidence in sample collection and for critical comments on the manuscript. We are also grateful to three reviewers for constructive criticisms on the manuscript resulting in an improved presentation of our ideas and results.

Received 18 November 1998; revised accepted 1 April 1999